ENVIRONMENTAL RESEARCH
LETTERS

LETTER • OPEN ACCESS

Projected response of global runoff to El Niño-Southern oscillation

ENVIRONMENTAL RESEARCH
LETTERS

LETTER

Projected response of global runoff to El Niño-Southern oscillation

Thanh Le[1], Kyung-Ja Ha[2,3,*] and Deg-Hyo Bae[1,*]

[1] Department of Civil and Environmental Engineering, Sejong University, Seoul 05006, Republic of Korea
[2] Center for Climate Physics, Institute for Basic Science, Busan, Republic of Korea
[3] Research Center for Climate Sciences and Department of Atmospheric Sciences, Pusan National University, Busan, Republic of Korea
* Authors to whom any correspondence should be addressed.

E-mail: kjha@pusan.ac.kr **and** dhbae@sejong.ac.kr

Keywords: future projections, El Niño-Southern oscillation, causal impacts, runoff, CMIP6

Supplementary material for this article is available online

OPEN ACCESS

RECEIVED
9 May 2021

REVISED
28 June 2021

ACCEPTED FOR PUBLICATION
13 July 2021

PUBLISHED
29 July 2021

Abstract

The El Niño-Southern Oscillation (ENSO) is a major mode of interannual climate variability and is expected to affect runoff variations at a global scale. While previous studies focused on the correlation analysis between ENSO and runoff and ENSO-induced amplitude changes of runoff, causal analysis considering the confounding impacts of other major climate modes is lacking. As more extreme ENSO events are projected in the future, it is crucial to enhance our understanding of the impacts of ENSO on global runoff. Here we examine the causal influences of ENSO on runoff over the future period 2015–2100 using outputs from Coupled Modeling Intercomparison Project Phase 6 model simulations. Our analyses account for the possible confounding effects of the Southern Annular Mode, the North Atlantic Oscillation and the Indian Ocean Dipole. We find that the signature of ENSO is detectable in future total runoff over various regions including limited areas in central and eastern Asia, large parts of Southeast Asia, limited areas in the eastern and southern Africa, western and eastern Australia, parts of southern and western North America, eastern Antarctica and large parts of South America. There is a high agreement across models for the causal influences of ENSO over central Asia, the eastern coast of Australia, southcentral North America and South America. Multi-model future projections demonstrate higher impacts of ENSO on total runoff over western and central Asia, the western coast of North America and southeastern South America compared to the historical period 1915–2000. All regions with substantial ENSO impacts account for 3.6% land-area in historical simulation and this fraction increases to 5.6% in the future scenario. In addition, the results underscore that surface runoff is less sensitive to ENSO compared to total runoff in most regions. These results may have implications for future water management planning based on ENSO.

1. Introduction

The El Niño-Southern Oscillation (ENSO; Bjerknes 1969) is a main mode of climate variability with worldwide influences (McPhaden *et al* 2006, Chen *et al* 2017, Cai *et al* 2020). ENSO affects precipitation (Sun *et al* 2020), winds (Yeh *et al* 2018) and evaporation (Martens *et al* 2018, Le and Bae 2020) and causes changes in water storage (Phillips *et al* 2012, Frappart *et al* 2018), drought (Trenberth *et al* 2014, Zambrano Mera *et al* 2018, Ault 2020) and water cycle extremes (Ward *et al* 2014, Emerton *et al* 2017) at a global scale. Nevertheless, uncertainty exists regarding the influences of ENSO on global runoff in the future periods under global warming, partly due to the ambiguities in the projections of hydroclimate in climate models (Knutti and Sedláček 2012) and the biases in runoff sensitivities (Lehner *et al* 2019).

Global streamflow is crucial for human health and ecosystems (Milly *et al* 2005, Patz *et al* 2005, De Graaf *et al* 2019, Jasechko *et al* 2021). Future runoff variations are important for evaluating the sustainability of future water resources availability as global warming is expected to increase regional heat waves (Dosio *et al* 2018, Seo *et al* 2021), wild fires (Turco *et al* 2018), hydroclimatic extremes (Kim and Bae 2020), droughts and flood risks (Alfieri *et al* 2017, Best 2019, Uhe *et al* 2019), frequency of sudden stratospheric

warmings and delay of seasonal transition (Rao and Garfinkel 2021a, 2021b) and causes an increase in human and economic losses (Dottori *et al* 2018). While runoff data can be used as a proxy for flooding, its variations can be affected by major modes of climate variability, including ENSO. In particular, ENSO was shown to have impacts on regional river discharge and flooding risks (Ward *et al* 2010, Munoz and Dee 2017), future Nile flow variations (Siam and Eltahir 2017) and runoff and sediments transport over Amazonia (Aalto *et al* 2003) and western Peruvian Andes (Morera *et al* 2017). Given that more extreme ENSO events are projected in the future (Cai *et al* 2014, Fredriksen *et al* 2020), it is necessary to enhance our understanding for the impacts of ENSO on global runoff.

Recent developments of earth system models where climate model and land model (Eyring *et al* 2016, Lawrence *et al* 2016, Van Den Hurk *et al* 2016) are coupled provide tools for systematically assessing the impacts of climate change on the regional hydrological cycle. Land model components in the current generation of earth system models in the Coupled Modeling Intercomparison Project Phase 6 (CMIP6) contribute important outputs to better understand the impacts of ENSO on future global runoff. As there are uncertainties across models in projections of ENSO (Taschetto *et al* 2014, Beobide-Arsuaga *et al* 2021, Tang *et al* 2021), it is also essential to assess the biases of CMIP6 models in simulating the connection between ENSO and future runoff.

In this study, we estimate the possibility for the influences of ENSO on runoff at a global scale. While an assessment for the causal impacts of ENSO on future runoff is necessary, it is also important to consider the simultaneous impacts of other modes of climate variability (e.g. the Southern Annular Mode (SAM), the Indian Ocean Dipole (IOD) and the North Atlantic Oscillation (NAO)) on runoff. We consider the consistency across CMIP6 models in projecting the response of runoff to ENSO.

2. Data and methods

2.1. Data

The data used in this study were taken from the Scenario Model Intercomparison Project (ScenarioMIP; O'Neill *et al* 2016) of the CMIP6 (Eyring *et al* 2016) and covers the 2015–2100 period. We limited our study to two future simulations of SSP2-4.5 (i.e. Shared Socio-Economic Pathway 2 and 2100 climate forcing level of 4.5 W m^{-2}) and SSP5-8.5 (i.e. Shared Socio-Economic Pathway 5 and 2100 climate forcing level of 8.5 W m^{-2}). Historical simulation (Eyring *et al* 2016) over the 1915–2000 period is used as a baseline to evaluate possible changes in the future influences of ENSO on global runoff compared to the earlier period. The list of the 15 CMIP6 models with available runoff data and employed in this study is shown in table S1. Additional information about the spatial resolution of the model in the atmosphere and a brief review of the difference between CMIP5/6 models can be found in a recent work (Rao and Garfinkel 2021a). The spatial resolution of the model in the atmosphere and over land surface are similar for each model. We mainly used monthly total runoff (variable 'mrro') and surface runoff (variable 'mrros') data. Surface runoff is the flow of water on the land surface when rainwater or snowmelt and other sources exceeds the infiltration capacity of the soil. Total runoff is considered as surface runoff plus drainage in soil or groundwater flow. We utilized monthly sea level pressure (SLP, variable 'psl') and sea surface temperature (SST, variable 'ts') to compute the time series of climate modes (see section 2.2 and text S1).

2.2. Methods

The methods used for evaluating the causal impacts of ENSO on global runoff are similar to the approach described in a recent study (Le and Bae 2020), which was based on a multivariate predictive model to test the null hypothesis of no Granger causality. This approach uses the probability value or *p*-value as a metric to evaluate the possibility for the absence of causal impacts of ENSO on runoff. Following recent guidance for quantifying the degree of uncertainty (Stocker *et al* 2013), we used the terms 'unlikely' and 'likely' for the 0%–33% and 66%–100% probability of the likelihood of the outcome, respectively. For instance, if the *p*-value is less than 0.33, the result implies that ENSO is unlikely to exhibit no Granger causality on runoff. In this case, we infer that ENSO has 'causal effect' on runoff.

We considered the confounding impacts of other major modes of climate variability (i.e. the IOD (Saji *et al* 1999, Webster *et al* 1999), the SAM (e.g. Cai *et al* 2011) and the NAO (Hurrell *et al* 2003)) on the connection between ENSO and runoff in the analyses. Although ENSO is the leading mode of climate variations, climate variability in the Atlantic and Indian oceans may have influences on the tropical Pacific (Cai *et al* 2011, 2019, Wurtzel *et al* 2018, Abram *et al* 2020, Le *et al* 2020), and thus, modulate the impacts of ENSO on global runoff. Therefore, analyses accounting for the confounding impacts of these climate modes provides realistic assessment for the response of global runoff to ENSO. The more specific information of the methods used is described in section text S1.

The ENSO index was computed as the average SST anomalies in the Niño 3.4 area (120–170°W; 5°N–5°S) in boreal winter (December–January–February, DJF). The DMI was given as the difference in boreal fall (September–October–November, SON) SST anomalies between two Indian Ocean regions of the western pole (50–70°E; 10°N–10°S) and southeastern pole (90–110°E; 0°N–10°S). The SAM was

calculated as the first empirical orthogonal function (EOF) of the boreal summer (June–July–August, JJA) SLP anomalies for the region of 40–70°S. The NAO index is computed as the EOF of boreal winter (DJF) SLP anomalies in the North Atlantic area (90°W–40°E, 20°–70°N).

3. Results and discussion

3.1. ENSO impacts on annual mean total and surface runoff

Based on the analysis of multi-model outputs, figure 1 shows the causal impacts of ENSO on global total runoff for the historical period 1915–2000 (a) and the future period 2015–2100 of the two scenarios SSP2-4.5 (b) and SSP5-8.5 (c). In figure 1, we show that ENSO is unlikely to exhibit no causal effects on total runoff (i.e. *p*-value were lower than 0.33 (Stocker *et al* 2013)) over various regions including limited areas in central and eastern Asia, large parts of Southeast Asia, limited areas in the eastern and southern Africa, western and eastern Australia, southern North America, much of South America and parts of eastern Antarctica. The pattern of projected causal impacts of ENSO on global runoff qualitatively resembles the pattern in the historical simulations. However, ENSO signals are relatively stronger in SSP2-4.5 compared to historical simulation and SSP5-8.5 where the impacts are expanded in North America and eastern Antarctica. Details for the influences of ENSO on total runoff over these areas for SSP2-4.5 are presented in figure S1 (available online at stacks.iop.org/ERL/16/084037/mmedia). We observe the nonsignificant and uncertain response of total runoff to ENSO over large parts of Europe, northern North America, eastern Asia, central Australia, central and northern Africa (figure 1).

Differences between projected and historical patterns of ENSO impacts on total runoff are apparent in several regions (figures 2(a) and (b)). Specifically, there is a possible intensification of ENSO impacts over western and central Asia, the western coast of North America (mainly SSP2-4.5) and southeastern South America. Conversely, we notice a minor reduction in the likelihood of the impacts of ENSO over Australia, south-central North America and northeastern South America. The changes in the pattern of ENSO impacts on global runoff imply that external forcing (i.e. changes in concentrations of greenhouse gases) may modulate the ENSO-induced runoff variations. These results also suggest a complex picture of ENSO impacts on future global runoff which is not merely associated with the rate of global warming. Figure 2(c) shows that the regions with substantial ENSO impacts on total runoff account for 5.6% of land area (i.e. 1.6% of total earth surface) for SSP2-4.5 and 3.5% of land area (i.e. 1% of total earth surface) for SSP5-8.5 scenario. The regions influenced by ENSO in historical simulation account for 3.6% of land area (i.e. 1% of total earth surface). These results imply an expansion of future ENSO effects on regional runoff, particularly regarding the SSP2-4.5 scenario.

Figure 3 reveals that the response of global surface runoff to ENSO is much weaker compared to the response of global total runoff. There are very few areas (i.e. limited regions of central Asia, Southeast Asia, Australia, North America, South America and Antarctica) in which ENSO is unlikely to show no causal effects on runoff (i.e. *p*-value were lower than 0.33). The results suggest that subsurface runoff might be more sensitive to ENSO variations compared to surface runoff. Particularly, ENSO impacts on surface runoff over Antarctica are stronger in both future scenarios SSP2-4.5 and SSP5-8.5 (figures 3(b) and (c)) compared to the historical simulation (figure 3(a)). Figure S2 shows that the land area influenced by ENSO in the SSP2-4.5 scenario is estimated at nearly 2.4% (or nearly 0.7% of total earth surface) while it is 1.5% (0.44%) for the historical simulation and 1.4% (0.41%) for SSP5-8.5 scenario.

3.2. The consistency of ENSO impacts on runoff

We observe high agreement between models for the significant causal effects of ENSO on total runoff over the regions of central and western Asia, western and eastern coast of Australia, parts of North America and South America (figures 1 and S1(a), (e), (c), (f) and (g)). The models agree well on the nonsignificant response of total runoff to ENSO over large parts of eastern Europe, northern North America, eastern Asia, central Australia, central and southern Africa (figure 1). The consistency across models for the impacts of ENSO on runoff over south-central North America, the western and eastern coast of Australia, parts of central Asia and South America (figure 1) may suggest the realism of hydrologic simulations over these regions. However, there is a low agreement between models over western Europe, northern Africa, large parts of central and eastern Asia, Southeast Asia and Antarctica.

Figure 4 details the results of 15 individual models (table S1) for the causal impacts of ENSO on global total runoff for the future scenario SSP2-4.5 over the 2015–2100 period. The results of these models for the historical experiment over the 1915–2000 period and the future scenario SSP5-8.5 over the 2015–2100 period are presented in Figures S3 and S4, respectively. In figure 4, several models overestimated the response of runoff to ENSO compared to the multi-model mean. For instance, the responses of runoff to ENSO over Africa are stronger in the models ACCESS_ESM1_5, CESM2_WACCM, IPSL-CM6A-LR, MPI_ESM1_2_HR and MPI_ESM1_2_LR. Several models (e.g. BCC_CSM2_MR, CESM2_WACCM, FGOALS_f3_L, MIROC6, MPI_ESM1_2_HR, MPI_ESM1_2_LR, MRI_ESM2_0 and

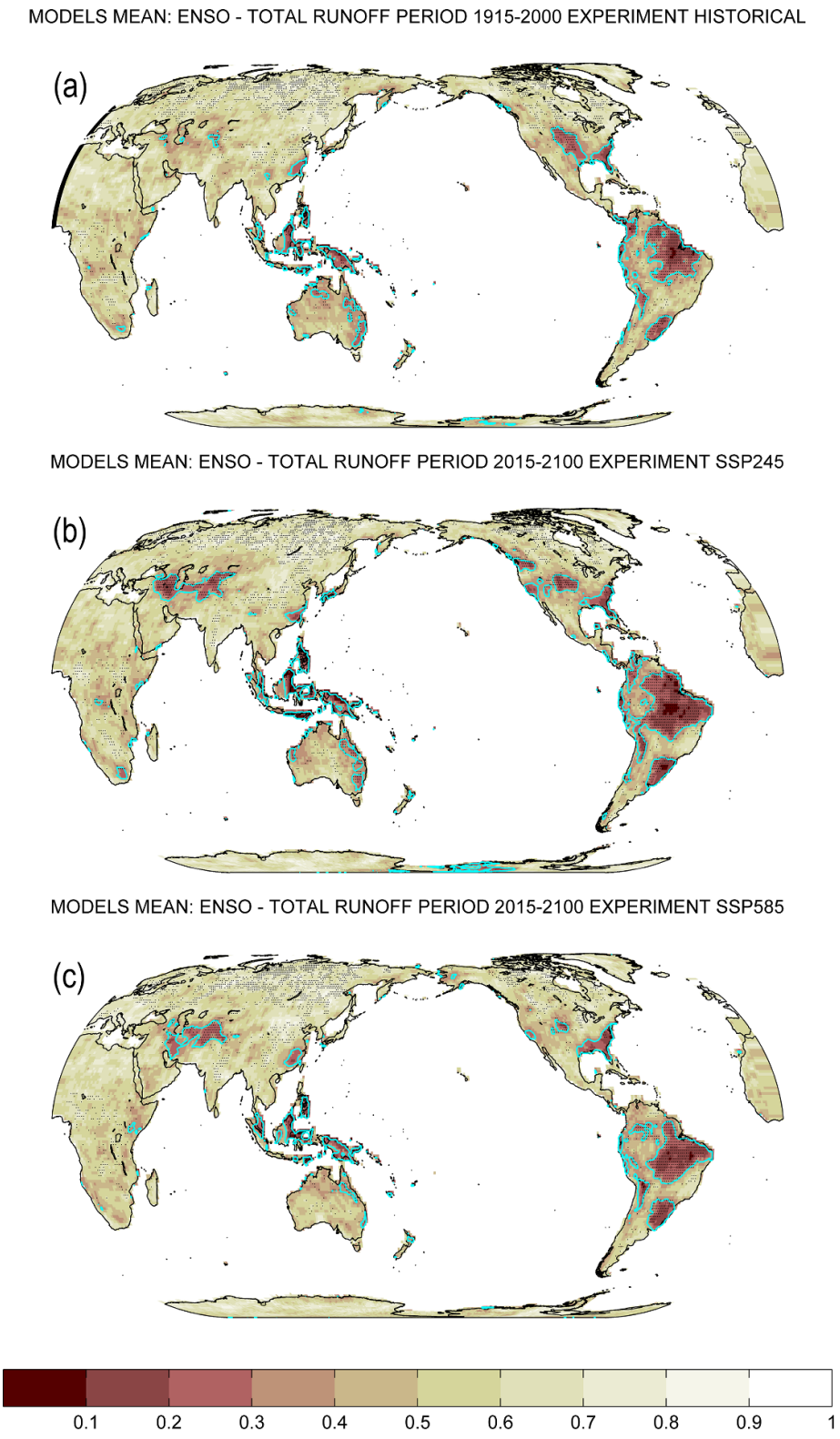

Figure 1. Map of multi-model mean probability for no Granger causality from ENSO to annual mean total runoff for the historical simulation of the 1915–2000 period (a) and the future scenarios SSP2-4.5 (b) and SSP5-8.5 (c) over the 2015–2100 period. Stippling shows that at least 70% of total models demonstrate agreement on the mean probability of all models at a given grid point. The agreement of a single model is defined when the difference between the selected model's probability and the multi-model mean probability is less than one standard deviation of the multi-model mean probability. The cyan contour line specifies $p = 0.33$. Brown shades imply a low probability for no Granger causality. ENSO: El Niño–Southern Oscillation.

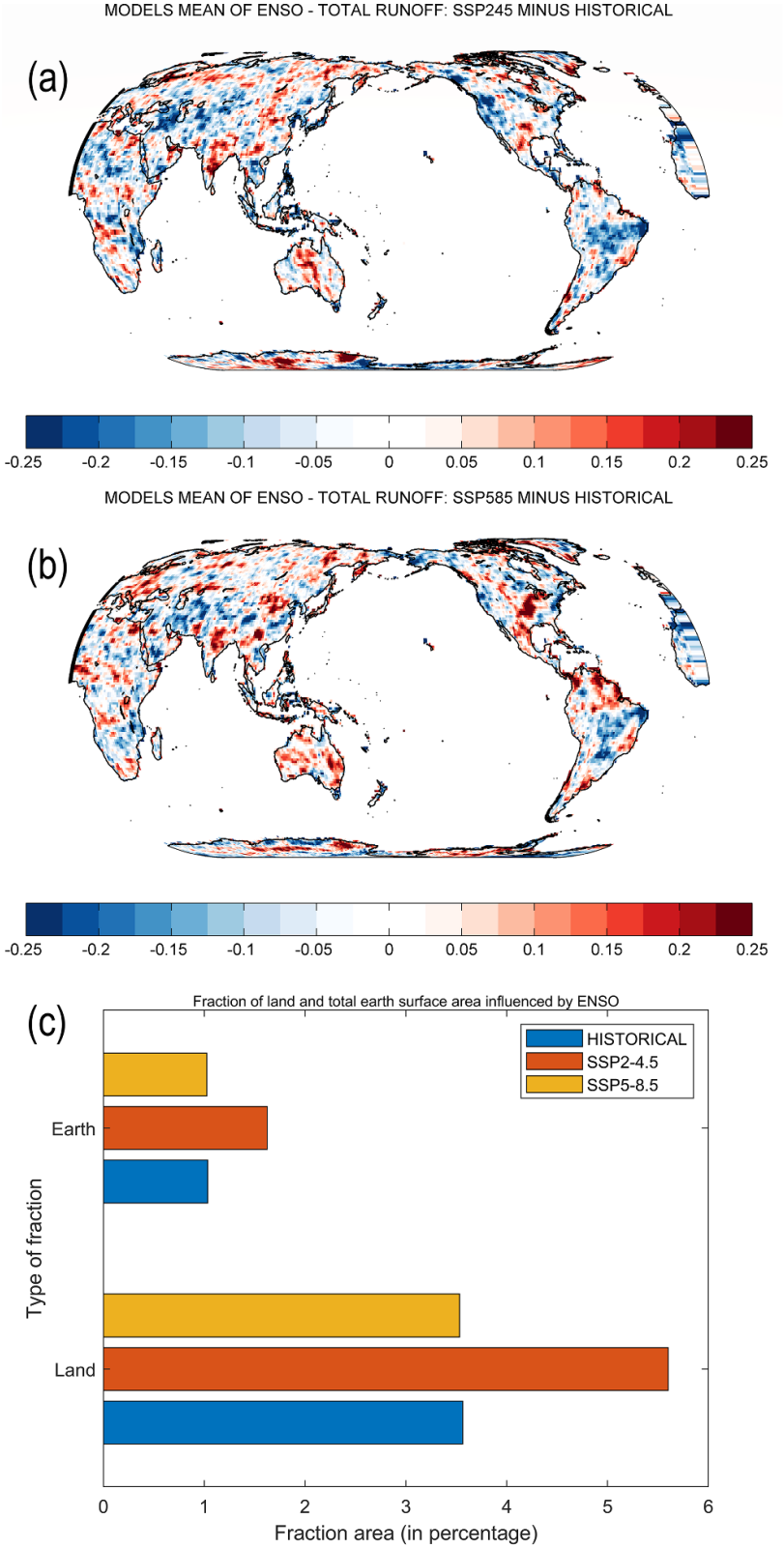

Figure 2. (a) Difference of multi-model mean probability for no Granger causality of ENSO on annual mean total runoff between future scenario SSP2-4.5 and historical experiment (i.e. SSP2-4.5 minus historical experiment). (b) Difference of multi-model mean probability for no Granger causality of ENSO on annual mean total runoff between future scenario SSP5-8.5 and historical experiment (i.e. SSP5-8.5 minus historical experiment). In (a) and (b), blue shades denote a lower probability of no Granger causality in the future scenario SSP2-4.5 (and SSP5-8.5) compared to the historical experiment. Brown shades signify a lower probability of no Granger causality in the historical experiment compared to the future scenario SSP2-4.5 (and SSP5-8.5). (c) Fraction of land and total Earth surface with probability for the absence of Granger causality from ENSO to runoff lower than 0.33 (i.e. $p < 0.33$). Fraction areas influenced by ENSO in the historical experiment and future scenarios SSP2-4.5 and SSP5-8.5 are presented in blue, red and yellow bars, respectively. ENSO: El Niño–Southern Oscillation.

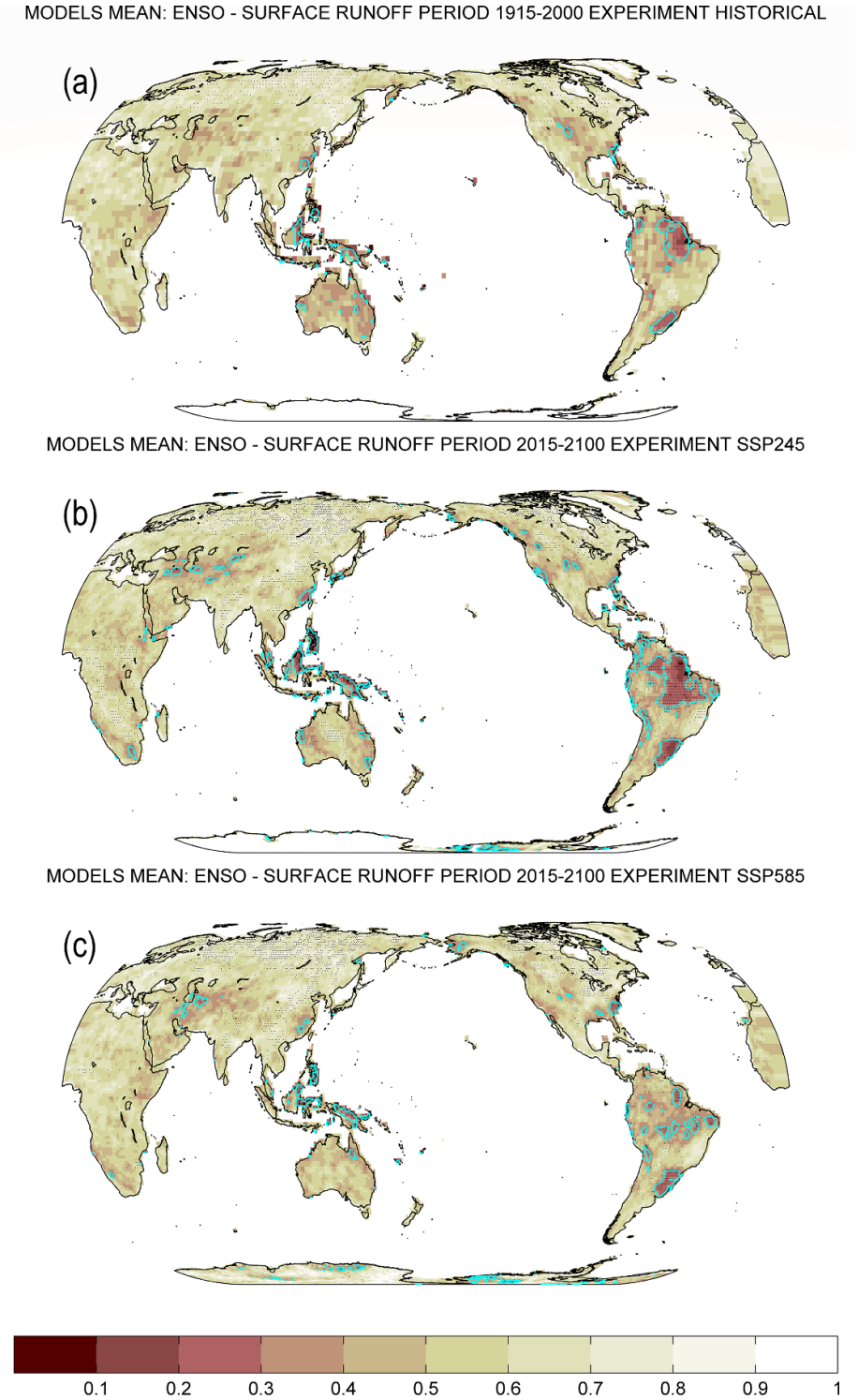

Figure 3. As in figure 1, but for the probability for the absence of Granger causality of ENSO on the annual mean surface (0–10 cm) runoff for the historical simulation of the 1915–2000 period (a) and the future scenarios SSP2-4.5 (b) and SSP5-8.5 (c) over the 2015–2100 period. ENSO: El Niño–Southern Oscillation.

UKESM1_0_LL) show a more sensitive response of runoff to ENSO over central and western Asia compared to others. Conversely, the response of runoff to ENSO over South America is weak in the models BCC_CSM2_MR, CNRM_CM6_1_HR and CNRM_ESM2_1 while most models show that ENSO is very unlikely (i.e. *p*-value were lower than 0.1) to have no causal effects on runoff over large parts of this region. Some models (i.e. BCC_CSM2_MR, ACCESS_ESM1_5, CESM2_WACCM, IPSL-CM6A-LR, MIROC6, MPI_ESM1_2_HR and MPI_ESM1_2_LR) show that ENSO is very unlikely (i.e. *p*-value were lower than 0.1) to have no causal effects on runoff over large parts of Australia, implying significant causal effects of ENSO in this area.

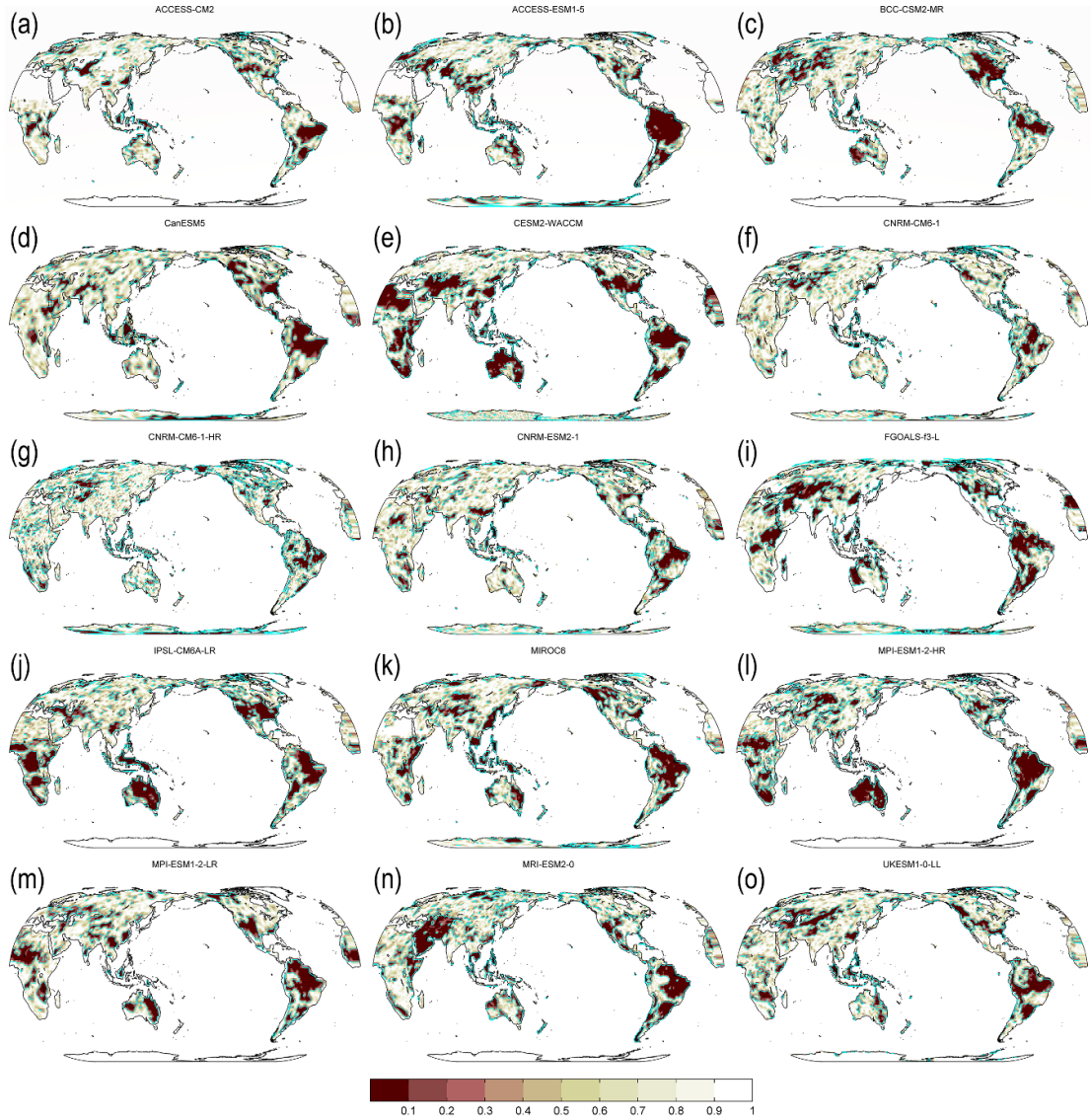

Figure 4. As in figure 1, but for the probability for no Granger causality of ENSO on annual mean total runoff for the future scenario SSP2-4.5 over the 2015–2100 period of 15 individual models (see also table S1). ENSO: El Niño–Southern Oscillation.

There is an overall lack of agreement for the impacts of ENSO on surface runoff for most regions (figure 3), suggesting a large spread of models in simulating the land-atmosphere interactions. The model biases also reflect the confounding impacts of various processes on regional runoff. In addition, model biases might be associated with errors in replicating the variations of ENSO (Taschetto *et al* 2014) and the IOD (Weller and Cai 2013, McKenna *et al* 2020) or the interactions between these two modes (Cai *et al* 2019, Le and Bae 2019, Le *et al* 2020).

3.3. ENSO impacts on seasonal mean total runoff

While ENSO peaks in boreal winter (DJF), its causal effects on total runoff are the most significant in the following boreal spring (MAM) and steadily decline during the following boreal summer (JJA), fall (SON) and winter (figure 5). Particularly, ENSO at year t [$D(t)$JF($t+1$)] is unlikely to exhibit no causal influences on spring [MAM($t+1$)] total runoff (i.e. p-value were lower than 0.33) over limited areas of northern Australia, Southeast Asia, parts of North America, limited areas over eastern Africa and eastern Asia, central and western Asia, and parts of South America (figure 5(a)). The regions with substantial ENSO impacts on spring total runoff account for 3.5% of land area (i.e. 1% of total earth surface, figure S5). In the following summer [JJA($t+1$)], ENSO [$D(t)$JF($t+1$)] impacts on total runoff are observed in limited areas of northern Australia, Southeast Asia and South America (figure 5(b)), accounting for 0.6% of land area (i.e. 0.17% of total earth surface, figure S5). In the following fall and winter [SON($t+1$) and $D(t+1)$JF($t+2$)], ENSO [$D(t)$JF($t+1$)] is likely to exhibit no causal influences on total runoff (i.e. p-value were higher than 0.66 (Stocker *et al* 2013)) for most areas (figures 5(c) and (d)). The impacted areas in the following fall and

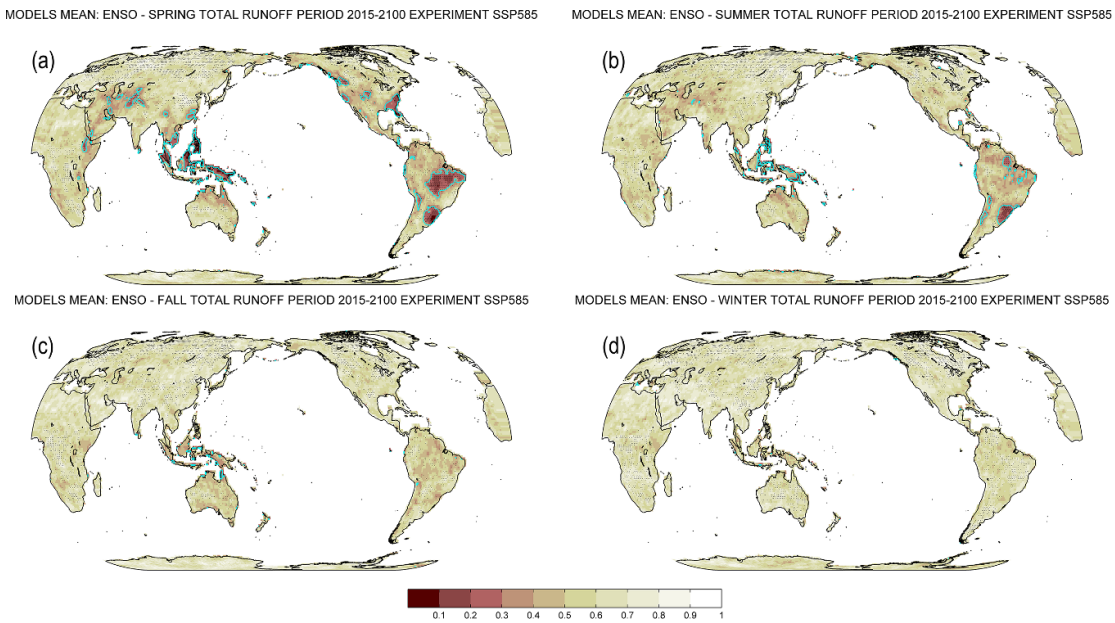

Figure 5. Map of multi-model mean probability for no Granger causality from ENSO [$D(t)$JF$(t+1)$] to seasonal mean total runoff for the future scenario SSP5-8.5 over the 2015–2100 period. (a) Spring [MAM$(t+1)$]. (b) Summer [JJA$(t+1)$]. (c) Fall [SON$(t+1)$]. (d) Winter [$D(t+1)$JF$(t+2)$]. Stippling shows that at least 70% of total models demonstrate agreement on the mean probability of all models at a given grid point. The cyan contour line specifies $p = 0.33$. Brown shades imply a low probability for no Granger causality. The results are similar for the future scenarios SSP2-4.5 (not shown). ENSO: El Niño–Southern Oscillation.

winter only account for less than 0.2% of land area (i.e. less than 0.05% of total earth surface, figure S5) although ENSO [$D(t)$JF$(t+1)$] impacts on total runoff may persist until the following fall [SON$(t+1)$] over very limited areas of Southeast Asia and northern Australia (figure 5(c)). These results suggest that spring [MAM$(t+1)$] and summer [JJA$(t+1)$] runoff predictability based on ENSO [$D(t)$JF$(t+1)$] might be more effective compared to other seasons.

3.4. Discussion

Biases of land models are increased when coupled with atmospheric models due to the complex connection between evapotranspiration and precipitation (Mizuochi *et al* 2021). While precipitation is a major driver of global runoff variations (Milly *et al* 2005, Piao *et al* 2007), climate models show large spread and uncertainty in simulating runoff, partly due to inconsistency in simulating changes in precipitation (Lehner *et al* 2019). Although increased precipitation does not necessarily enhance runoff and surface water availability (Ha *et al* 2020), the effects of changes in precipitation on runoff variations may be more important compared to the effects of changes in land use and evaporation (Teuling *et al* 2019). Despite the biases in runoff sensitivities to temperature and precipitation (Lehner *et al* 2019), our results for the impacts of ENSO on global runoff (figures 1 and S1) are synchronous with the impacts of ENSO on global evaporation (Martens *et al* 2018, Le and Bae 2020) and soil moisture over various regions. While precipitation and evaporation play an important role in future global water availability (Ha *et al* 2020, Konapala *et al* 2020), these two variables are influenced by ENSO (Le and Bae 2020, Sun *et al* 2020) via ENSO-induced changes of Walker circulation over the tropics and stationary Rossby wave trains over extratropical regions (Dai and Wigley 2000, Cai *et al* 2020). Hence, ENSO signatures on hydroclimate variations over central and eastern Asia, Southeast Asia, Australia, parts of North America and much of South America are robust.

In particular, the substantial effects of ENSO on runoff over South America (figures 1 and S1(g)) show an agreement with previous studies (Malhi *et al* 2008, Grimm and Tedeschi 2009, Cai *et al* 2020) which suggested a pattern of floods in the western coast and droughts in the Amazonia and the northeastern part of the continent during El Niño phase. The significant response of (both total and surface) runoff to ENSO in eastern Antarctica but with low consistency across models (figures 1 and S1(h)) may require further investigations using higher resolution models as these influences might be crucial for the regional ecosystem in a warming environment. The expansion of ENSO impacts on total runoff over western and central Asia in the future scenarios SSP2-4.5 and SSP5-8.5 (figures 1(b) and (c)) is in agreement with the significant response of precipitation and evaporation to ENSO in these regions (Le and Bae 2020). In addition, the higher impacts of ENSO in the SSP2-4.5 scenario compared to SSP5-8.5 scenario (figures 1(b) and (c)) might be associated with the decrease in anthropogenic influences on natural runoff and increase

in ENSO impacts on regional precipitation. Natural climate variability and human activities are the two major factors of hydrological changes. As the impacts of human activities on terrestrial hydrology might be of similar magnitude compared to the impacts of changing precipitation and temperature (Ferguson and Maxwell 2012), changes in land-use scenarios may affect the causal impacts of ENSO on runoff. The land use pathways used in SSP2-4.5 are less extreme compared to other SSPs including SSP5-8.5 (O'Neill *et al* 2016). For instance, the global time series of pastureland area is higher while irrigated cropland area is significantly lower in SSP2-4.5 compared to SSP5-8.5 (Lawrence *et al* 2016). Hence, it is expected that the impacts of human activities on hydrological changes are weaker in SSP2-4.5 compared to SSP5-8.5, leading to a possible difference in the causal impacts of ENSO on global runoff in these two scenarios.

We observe limited and uncertain effects of ENSO on runoff over eastern and southern Africa (figure 1), consistent with a recent study suggesting a complex pathway for the impacts of ENSO on these areas (Siderius *et al* 2018). The weak response of runoff to ENSO over Europe might be due to the dominant influence of the NAO (Hurrell *et al* 2003) and the East Atlantic pattern (Nobre *et al* 2017) in this region. The weaker response of surface runoff to ENSO compared to total runoff (figures 1 and 3) might be due to the vertical gradient of changes in soil moisture where more negative changes are observed near the surface (Berg *et al* 2017). In addition, these distinct sensitivities might be due to differences of human impacts on surface runoff and subsurface drainage via land use activities which potentially reduce the influences of ENSO at a regional scale.

The land area affected by ENSO (figures 2(c), S2 and S5) might be less than expected compared to previous study using correlation analysis (Ward *et al* 2014). In the correlation analysis between ENSO and runoff and flood risk, the confounding impacts of other climate modes might not be considered, leading to higher influence of ENSO. In addition, the low fraction of land area affected by ENSO is due to the human controls of runoff (Best 2019, De Graaf *et al* 2019) in major river systems (e.g. via dams building, groundwater pumping and irrigation systems). The impacts of human activities associated with potential changes in runoff are incorporated in earth system models via the unique impacts of land-use activities and land-cover changes (Lawrence *et al* 2016, O'Neill *et al* 2016, Van Den Hurk *et al* 2016). These anthropogenic impacts result in lower causal effects of ENSO (figure 1) and other natural climate variability on runoff in the largest river basins. For example, in figure 1, ENSO is likely to have no causal impacts on the Huang He (Yellow) river basin in the eastern Asia, the Nile river basin in the northeastern Africa and the Mekong river basin in the Southeastern Asia.

Figure S6 depicts the normalized time series (i.e. standard deviation $\sigma = 1$) of ENSO in the models of the future scenarios SSP2-4.5 and SSP5-8.5 for the years 2015–2100. The projected variations of ENSO-amplitude are consistent between models with the amplitude is mostly in the range from -3σ to $+3\sigma$. However, the timing of strong positive ENSO events (exceeding $+1.5\sigma$ and approaching $+3\sigma$; figure S6) and strong negative ENSO events (falling below -1.5σ and approaching -3σ; figure S6) are different across models. The models CanESM5 and MRI_ESM2_0 exhibit rare cases of extreme ENSO events (i.e. ENSO index higher than $+3\sigma$ or lower than -3σ; figure S6(a)) while these extreme ENSO events are not apparent in other models. Recent works (Fredriksen *et al* 2020, Beobide-Arsuaga *et al* 2021) suggested a large spread of projections of ENSO characteristics across CMIP6 models. Thus, future change of ENSO properties (i.e. ENSO intensity, frequency, and location) may contribute to the uncertainties of ENSO impacts on global runoff.

As CMIP6 models show capability in reproducing variations of extreme runoff (Villarini and Zhang 2020) and ENSO might increase flood risks through its impacts on surface water storage (Munoz and Dee 2017), the use of major climate modes may improve the prediction of seasonal peak flows (Lee *et al* 2018).

4. Summary and conclusions

In this work, we evaluated the causal impacts of ENSO on global runoff over the 21st century using outputs from CMIP6 models. Our results demonstrated that ENSO is likely to exhibit some causal influences on total runoff over various regions including limited areas in central and eastern Asia, large parts of Southeast Asia, limited areas in the eastern and southern Africa, western and eastern Australia, southern North America, much of South America and parts of eastern Antarctica (figures 1 and S1). The response of total runoff to ENSO is robust and consistent across models in SSP2-4.5 and SSP5-8.5, particularly regarding the areas of central and western Asia, western and eastern coast of Australia, parts of North America and South America. However, there is a low agreement between models over western Europe, northern Africa, large parts of central and eastern Asia, Southeast Asia and Antarctica. As Southeast Asia is a focused area for studies of biodiversity, human-climate interactions, land surface change and wildfire with a dense population and plays an important role in the detection, mitigation, and adaptation of global change, improved models' accuracy for the ENSO-induced changes of runoff over this region may benefit for regional economy, biodiversity and ecosystem.

We find an expansion of ENSO impacts on total runoff over western and central Asia in the future scenarios SSP2-4.5 and SSP5-8.5 compared to the historical simulation (figures 2(a) and (b)). Conversely,

there is a decrease in ENSO signature over south-central North America, northeastern South America and Australia in the SSP5-8.5 scenario compared to the historical simulation. Future works may assess the changes in amplitude of runoff to further constraint the contribution of ENSO on regional water resources availability. As precipitation is the main driver of runoff variations, further understanding of the impacts of ENSO on precipitation may reduce the uncertainties of future ENSO-induced hydrological changes. Additional information on the impacts of ENSO during its developing and decaying seasons (e.g. JJA and SON) on runoff might be helpful for future water resources management.

Data Availability Statement

The data that support the findings of this study are openly available at the following URL/DOI: https://esgf-node.llnl.gov/search/cmip6/.

Acknowledgments

The authors thank the anonymous reviewers for their valuable comments and suggestions. We acknowledge the World Climate Research Programme, which through its Working Group on Coupled Modelling, coordinated and promoted CMIP6. We thank the climate modelling groups (listed in table S1) for producing and making available their model output, the Earth System Grid Federation (ESGF) for archiving the data and providing access, and the multiple funding agencies who support CMIP6 and ESGF. K J Ha and T Le are supported by the National Research Foundation of Korea (NRF) grant funded by the Korea government (MSIT) (Grant No. 2020R1A2C2006860 and Grant No. 2021R1G1A1004389).

ORCID iDs

Thanh Le https://orcid.org/0000-0001-5809-2751
Kyung-Ja Ha https://orcid.org/0000-0003-1753-9304

References

Aalto R, Maurice-Bourgoin L, Dunne T, Montgomery D R, Nittrouer C A and Guyot J-L 2003 Episodic sediment accumulation on Amazonian flood plains influenced by El Niño/Southern oscillation *Nature* **425** 493–7

Abram N J *et al* 2020 Coupling of Indo-Pacific climate variability over the last millennium *Nature* **579** 385–92

Alfieri L, Bisselink B, Dottori F, Naumann G, De Roo A, Salamon P, Wyser K and Feyen L 2017 Global projections of river flood risk in a warmer world *Earth's Futur* **5** 171–82

Ault T R 2020 On the essentials of drought in a changing climate *Science* **368** 256–60

Beobide-Arsuaga G, Bayr T, Reintges A and Latif M 2021 Uncertainty of ENSO-amplitude projections in CMIP5 and CMIP6 models *Clim. Dyn.* **56** 3875–88

Berg A, Sheffield J and Milly P C D 2017 Divergent surface and total soil moisture projections under global warming *Geophys. Res. Lett.* **44** 236–44

Best J 2019 Anthropogenic stresses on the world's big rivers *Nat. Geosci.* **12** 7–21

Bjerknes J 1969 Atmospheric teleconnections from the equatorial pacific 1 *Mon. Weather Rev.* **97** 163–72

Cai W *et al* 2014 Increasing frequency of extreme El Niño events due to greenhouse warming *Nat. Clim. Change* **5** 1–6

Cai W *et al* 2019 Pantropical climate interactions *Science* **363** eaav4236

Cai W *et al* 2020 Climate impacts of the El Niño–Southern Oscillation on South America *Nat. Rev. Earth Environ.* **1** 215–31

Cai W, Sullivan A and Cowan T 2011 Interactions of ENSO, the IOD, and the SAM in CMIP3 models *J. Clim.* **24** 1688–704

Chen Y, Morton D C, Andela N, Van Der Werf G R, Giglio L and Randerson J T 2017 A pan-tropical cascade of fire driven by El Niño/Southern Oscillation *Nat. Clim. Change* **7** 906–11

Dai A and Wigley T M L 2000 Global patterns of ENSO-induced precipitation *Geophys. Res. Lett.* **27** 1283–6

De Graaf I E M, Gleeson T, (Rens) Van Beek L P H, Sutanudjaja E H and Bierkens M F P 2019 Environmental flow limits to global groundwater pumping *Nature* **574** 90–4

Dosio A, Mentaschi L, Fischer E M and Wyser K 2018 Extreme heat waves under 1.5 °C and 2 °C global warming *Environ. Res. Lett.* **13** 054006

Dottori F *et al* 2018 Increased human and economic losses from river flooding with anthropogenic warming *Nat. Clim. Change* **8** 781–6

Emerton R, Cloke H L, Stephens E M, Zsoter E, Woolnough S J and Pappenberger F 2017 Complex picture for likelihood of ENSO-driven flood hazard *Nat. Commun.* **8** 1–9

Eyring V, Bony S, Meehl G A, Senior C A, Stevens B, Stouffer R J and Taylor K E 2016 Overview of the coupled model intercomparison project phase 6 (CMIP6) experimental design and organization *Geosci. Model Dev.* **9** 1937–58

Ferguson I M and Maxwell R M 2012 Human impacts on terrestrial hydrology: climate change versus pumping and irrigation *Environ. Res. Lett.* **7** 044022

Frappart F *et al* 2018 Influence of recent climatic events on the surface water storage of the Tonle Sap Lake *Sci. Total Environ.* **636** 1520–33

Fredriksen H B, Berner J, Subramanian A C and Capotondi A 2020 How does El Niño–Southern oscillation change under global warming—a first look at CMIP6 *Geophys. Res. Lett.* **47** 1–9

Grimm A M and Tedeschi R G 2009 ENSO and extreme rainfall events in South America *J. Clim.* **22** 1589–609

Ha K, Moon S, Timmermann A and Kim D 2020 Future changes of summer monsoon characteristics and evaporative demand over Asia in CMIP6 simulations *Geophys. Res. Lett.* **47** 1–10

Hurrell J W, Kushnir Y, Ottersen G and Visbeck M 2003 An overview of the North Atlantic Oscillation *Geophys. Monogr. Am. Geophys. Union* 1–35

Jasechko S, Seybold H, Perrone D, Fan Y and Kirchner J W 2021 Widespread potential loss of streamflow into underlying aquifers across the USA *Nature* **591** 391–5

Kim J-B and Bae D-H 2020 Intensification characteristics of hydroclimatic extremes in the Asian monsoon region under 1.5 and 2.0 °C of global warming *Hydrol. Earth Syst. Sci.* **24** 5799–820

Knutti R and Sedláček J 2012 Robustness and uncertainties in the new CMIP5 climate model projections *Nat. Clim. Change* **3** 369–73

Konapala G, Mishra A K, Wada Y and Mann M E 2020 Climate change will affect global water availability through compounding changes in seasonal precipitation and evaporation *Nat. Commun.* **11** 1–10

Lawrence D M *et al* 2016 The land use model intercomparison project (LUMIP) contribution to CMIP6: rationale and experimental design *Geosci. Model Dev.* **9** 2973–98

Le T and Bae D-H H 2019 Causal links on interannual timescale between ENSO and the IOD in CMIP5 future simulations *Geophys. Res. Lett.* **46** 1–9
Le T and Bae D-H 2020 Response of global evaporation to major climate modes in historical and future coupled model intercomparison project phase 5 simulations *Hydrol. Earth Syst. Sci.* **24** 1131–43
Le T, Ha K-J, Bae D-H and Kim S-H 2020 Causal effects of Indian ocean dipole on El Niño–Southern Oscillation during 1950–2014 based on high-resolution models and reanalysis data *Environ. Res. Lett.* **15** 1040b6
Lee D, Ward P and Block P 2018 Attribution of large-scale climate patterns to seasonal peak-flow and prospects for prediction globally *Water Resour. Res.* **54** 916–38
Lehner F, Wood A W, Vano J A, Lawrence D M, Clark M P and Mankin J S 2019 The potential to reduce uncertainty in regional runoff projections from climate models *Nat. Clim. Change* **9** 926–33
Malhi Y, Roberts J T, Betts R A, Killeen T J, Li W and Nobre C A 2008 Climate change, deforestation, and the fate of the Amazon *Science* **319** 169–72
Martens B, Waegeman W, Dorigo W A, Verhoest N E C and Miralles D G 2018 Terrestrial evaporation response to modes of climate variability *npj Clim. Atmos. Sci.* **1** 43
McKenna S, Santoso A, Gupta A S, Taschetto A S and Cai W 2020 Indian Ocean Dipole in CMIP5 and CMIP6: characteristics, biases, and links to ENSO *Sci. Rep.* **10** 11500
McPhaden M J, Zebiak S E and Glantz M H 2006 ENSO as an integrating concept in earth science *Science* **314** 1740–5
Milly P C D, Dunne K A and Vecchia A V 2005 Global pattern of trends in streamflow and water availability in a changing climate *Nature* **438** 347–50
Mizuochi H, Ducharne A, Cheruy F, Ghattas J, Al-Yaari A, Wigneron J-P, Bastrikov V, Peylin P, Maignan F and Vuichard N 2021 Multivariable evaluation of land surface processes in forced and coupled modes reveals new error sources to the simulated water cycle in the IPSL (Institute Pierre Simon Laplace) climate model *Hydrol. Earth Syst. Sci.* **25** 2199–221
Morera S B, Condom T, Crave A, Steer P and Guyot J L 2017 The impact of extreme El Niño events on modern sediment transport along the western Peruvian Andes (1968–2012) *Sci. Rep.* **7** 1–14
Munoz S E and Dee S G 2017 El Niño increases the risk of lower Mississippi River flooding *Sci. Rep.* **7** 1–7
Nobre G G, Jongman B, Aerts J and Ward P J 2017 The role of climate variability in extreme floods in Europe *Environ. Res. Lett.* **12** 084012
O'Neill B C *et al* 2016 The scenario model intercomparison project (ScenarioMIP) for CMIP6 *Geosci. Model Dev.* **9** 3461–82
Patz J A, Campbell-Lendrum D, Holloway T and Foley J A 2005 Impact of regional climate change on human health *Nature* **438** 310–7
Phillips T, Nerem R S, Fox-Kemper B, Famiglietti J S and Rajagopalan B 2012 The influence of ENSO on global terrestrial water storage using GRACE *Geophys. Res. Lett.* **39** L16705
Piao S, Friedlingstein P, Ciais P, De Noblet-ducoudre N, Labat D and Zaehle S 2007 Changes in climate and land use have a larger direct impact than rising CO2 on global river runoff trends *Proc. Natl Acad. Sci.* **104** 15242–7
Rao J and Garfinkel C I 2021a CMIP5/6 models project little change in the statistical characteristics of sudden stratospheric warmings in the 21st century *Environ. Res. Lett.* **16** 034024
Rao J and Garfinkel C I 2021b Projected changes of stratospheric final warmings in the Northern and Southern Hemispheres by CMIP5/6 models *Clim. Dyn.* **56** 3353–71
Saji N H, Goswami B N, Vinayachandran P N and Yamagata T 1999 A dipole mode in the tropical Indian Ocean *Nature* **401** 360–3
Seo Y-W, Ha K-J and Park T-W 2021 Feedback attribution to dry heatwaves over East Asia *Environ. Res. Lett.* **16** 064003
Siam M S and Eltahir E A B 2017 Climate change enhances interannual variability of the Nile river flow *Nat. Clim. Change* **7** 350–4
Siderius C, Gannon K E, Ndiyoi M, Opere A, Batisani N, Olago D, Pardoe J and Conway D 2018 Hydrological response and complex impact pathways of the 2015/2016 El Niño in Eastern and Southern Africa *Earth's Futur* **6** 2–22
Stocker T F *et al* 2013 Technical summary *Climate Change 2013—The Physical Science Basis* ed Intergovernmental Panel on Climate Change (Cambridge: Cambridge University Press) pp 31–116
Sun Q, Miao C, AghaKouchak A, Mallakpour I, Ji D and Duan Q 2020 Possible increased frequency of ENSO-related dry and wet conditions over some major watersheds in a warming climate *Bull. Am. Meteorol. Soc.* **101** E409–26
Tang T, Luo -J-J, Peng K, Qi L and Tang S 2021 Over-projected Pacific warming and extreme El Niño frequency due to CMIP5 common biases *Natl Sci. Rev.* nwab056
Taschetto A S, Gupta A S, Jourdain N C, Santoso A, Ummenhofer C C and England M H 2014 Cold tongue and warm pool ENSO events in CMIP5: mean state and future projections *J. Clim.* **27** 2861–85
Teuling A J, De Badts E A G, Jansen F A, Fuchs R, Buitink J, Hoek Van Dijke A J and Sterling S M 2019 Climate change, reforestation/afforestation, and urbanization impacts on evapotranspiration and streamflow in Europe *Hydrol. Earth Syst. Sci.* **23** 3631–52
Trenberth K E, Dai A, Van Der Schrier G, Jones P D, Barichivich J, Briffa K R and Sheffield J 2014 Global warming and changes in drought *Nat. Clim. Change* **4** 17–22
Turco M, Rosa-Cánovas J J, Bedia J, Jerez S, Montávez J P, Llasat M C and Provenzale A 2018 Exacerbated fires in Mediterranean Europe due to anthropogenic warming projected with non-stationary climate-fire models *Nat. Commun.* **9** 1–9
Uhe P F, Mitchell D M, Bates P D, Sampson C C, Smith A M and Islam A S 2019 Enhanced flood risk with 1.5 °C global warming in the Ganges–Brahmaputra–Meghna basin *Environ. Res. Lett.* **14** 074031
Van Den Hurk B *et al* 2016 LS3MIP (v1.0) contribution to CMIP6: the land surface, snow and soil moisture model intercomparison project—aims, setup and expected outcome *Geosci. Model Dev.* **9** 2809–32
Villarini G and Zhang W 2020 Projected changes in flooding: a continental U.S. perspective *Ann. New York Acad. Sci.* **1472** 95–103
Ward P J, Beets W, Bouwer L M, Aerts J C J H and Renssen H 2010 Sensitivity of river discharge to ENSO *Geophys. Res. Lett.* **37** L12402
Ward P J, Jongman B, Kummu M, Dettinger M D, Weiland F C S and Winsemius H C 2014 Strong influence of El Niño Southern Oscillation on flood risk around the world *Proc. Natl Acad. Sci. USA* **111** 15659–64
Webster P J, Moore A M, Loschnigg J P and Leben R R 1999 Coupled ocean–atmosphere dynamics in the Indian Ocean during 1997–98 *Nature* **401** 356–60
Weller E and Cai W 2013 Realism of the Indian ocean dipole in CMIP5 models: the implications for climate projections *J. Clim.* **26** 6649–59
Wurtzel J B, Abram N J, Lewis S C, Bajo P, Hellstrom J C, Troitzsch U and Heslop D 2018 Tropical Indo-Pacific hydroclimate response to North Atlantic forcing during the last deglaciation as recorded by a speleothem from Sumatra, Indonesia *Earth Planet. Sci. Lett.* **492** 264–78
Yeh S-W *et al* 2018 ENSO atmospheric teleconnections and their response to greenhouse gas forcing *Rev. Geophys.* **56** 185–206
Zambrano Mera Y E, Rivadeneira Vera J F and Pérez-Martín M Á 2018 Linking El Niño Southern Oscillation for early drought detection in tropical climates: the Ecuadorian coast *Sci. Total Environ.* **643** 193–207